



VU Research Portal

Spatial updating across saccades during manual interception

Dessing, J.C.; Crawford, J.D.; Medendorp, W.P.

published in

Journal of Vision
2011

DOI (link to publisher)

[10.1167/11.10.4](https://doi.org/10.1167/11.10.4)

document version

Publisher's PDF, also known as Version of record

[Link to publication in VU Research Portal](#)

citation for published version (APA)

Dessing, J. C., Crawford, J. D., & Medendorp, W. P. (2011). Spatial updating across saccades during manual interception. *Journal of Vision*, 11(10), 1-18. [4]. <https://doi.org/10.1167/11.10.4>

General rights

Copyright and moral rights for the publications made accessible in the public portal are retained by the authors and/or other copyright owners and it is a condition of accessing publications that users recognise and abide by the legal requirements associated with these rights.

- Users may download and print one copy of any publication from the public portal for the purpose of private study or research.
- You may not further distribute the material or use it for any profit-making activity or commercial gain
- You may freely distribute the URL identifying the publication in the public portal ?

Take down policy

If you believe that this document breaches copyright please contact us providing details, and we will remove access to the work immediately and investigate your claim.

E-mail address:

vuresearchportal.ub@vu.nl

Spatial updating across saccades during manual interception

Joost C. Dessing

Donders Institute for Brain, Cognition and Behaviour,
Radboud University Nijmegen, Nijmegen, The Netherlands,
Centre for Vision Research, York University, Toronto, Canada,
Research Institute MOVE, Faculty of Human Movement
Sciences, VU University, Amsterdam, The Netherlands, &
Canadian Action and Perception Network, Canada



J. Douglas Crawford

Centre for Vision Research, York University, Toronto, Canada,
Canadian Action and Perception Network, Canada, &
Departments of Psychology, Biology, and Kinesiology and
Health Sciences, and Neuroscience Graduate Diploma
Program, York University, Toronto, Canada



W. Pieter Medendorp

Donders Institute for Brain, Cognition and Behaviour,
Radboud University Nijmegen, Nijmegen, The Netherlands



We studied the effect of intervening saccades on the manual interception of a moving target. Previous studies suggest that stationary reach goals are coded and updated across saccades in gaze-centered coordinates, but whether this generalizes to interception is unknown. Subjects ($n = 9$) reached to manually intercept a moving target after it was rendered invisible. Subjects either fixated throughout the trial or made a saccade before reaching (both fixation points were in the range of -10° to 10°). Consistent with previous findings and our control experiment with stationary targets, the interception errors depended on the direction of the remembered moving goal relative to the new eye position, as if the target is coded and updated across the saccade in gaze-centered coordinates. However, our results were also more variable in that the interception errors for more than half of our subjects also depended on the goal direction relative to the initial gaze direction. This suggests that the feedforward transformations for interception differ from those for stationary targets. Our analyses show that the interception errors reflect a combination of biases in the (gaze-centered) representation of target motion and in the transformation of goal information into body-centered coordinates for action.

Keywords: interception, eye movements, visuomotor transformations, motion—2D, spatial vision

Citation: Dessing, J. C., Crawford, J. D., & Medendorp, W. P. (2011). Spatial updating across saccades during manual interception. *Journal of Vision*, 11(10):4, 1–18, <http://www.journalofvision.org/content/11/10/4>, doi:10.1167/11.10.4.

Introduction

Manual interception of a moving visual target requires sophisticated spatiotemporal control to steer the hand to the right place at the right time. When the target moves rapidly, or disappears from view, the brain must employ open-loop transformations to account for future target motion in order to overcome the delay in the visuomotor coupling. The pertinent mechanisms must rely on visual target motion, likely in combination with internal models of the body and world (Brouwer, Smeets, & Brenner, 2005; Dessing, Oostwoud Wijdenes, Peper, & Beek, 2009a; McIntyre, Zago, Berthoz, & Lacquaniti, 2001; Soechting & Flanders, 2008; Zago, McIntyre, Senot, & Lacquaniti, 2009).

While the kinematic characteristics of interception have been studied extensively (e.g., Beek, Dessing, Peper, &

Bullock, 2003; Savelsbergh, Whiting, & Bootsma, 1991; Zago et al., 2009), the neural computations and spatial transformations for interception have remained largely unexplored (Dessing, Peper, Bullock, & Beek, 2005; Merchant, Zarco, Prado, & Pérez, 2009). As in reaching toward stationary targets (Crawford, Medendorp, & Marrotta, 2004), interception requires that target motion signals, which necessarily enter the brain in a retina-based, gaze-centered sensory reference frame, are at some stage transformed into a muscle-based, body-centered reference frame for action (Blohm & Lefèvre, 2010). However, in contrast to the many studies of reaching and pointing (Crawford, Henriques, & Medendorp, 2011; Crawford et al., 2004; Medendorp, 2011), the intermediate reference frames and transformations for interception remain to be studied.

Manipulations of gaze direction during interception may reveal insights into the nature of these spatial

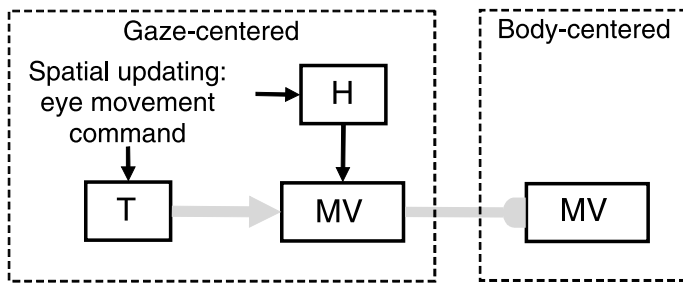


Figure 1. Simplified diagram of an essential part of the visuomotor transformation for reaching. Gaze-centered representations of target position (T) and hand position (H) are combined to calculate the gaze-centered movement vector (MV), which is subsequently transformed into a body-centered reference frame. While different diagrams can be envisioned, the main point of this figure is to illustrate the difference between representation and transformation biases. Representation biases are present in the target-related inputs to MV (gray arrow), while transformation biases arise in transforming the MV to body-centered coordinates (gray connector). For stationary targets, pointing errors have been argued to mainly reflect transformation biases, but for moving targets, representational biases may be present in target motion signals. In this figure, gaze-centered representations are updated across eye movements (black arrows from eye movement command).

representations. For example, studies with world-stationary targets have shown that reaches systematically overestimate the direction of the target relative to gaze (Beurze, Van Pelt, & Medendorp, 2006; Bock, 1986; Enright, 1995; Henriques & Crawford, 2000; McGuire & Sabes, 2009; Medendorp & Crawford, 2002). When a saccade intervenes between viewing the target and reaching for its remembered location, the resulting reach errors depend on the post-saccadic rather than pre-saccadic direction of the target relative to gaze (Henriques, Klier, Smith, Lowy, & Crawford, 1998; Van Pelt & Medendorp, 2008; Vaziri, Diedrichsen, & Shadmehr, 2006). Because the reach overshoot arises even when subjects initially fixate the target (and thus can most accurately represent it), the error does not reflect a bias in the initial sensory-derived representation of the target, i.e., it is not a “representation bias”. Rather, the error is thought to arise during the reference frame transformations that are involved in reaching (Beurze et al., 2006; Henriques et al., 1998; McGuire & Sabes, 2009; Figure 1). The dependency on the post-saccadic eccentricity suggests that the initial (gaze-centered) representation is updated across the saccade before the (post-saccadic) “transformation bias” arises. Similar reach errors have been observed under a variety of conditions and for targets presented in a variety of modalities (Byrne, Cappadocia, & Crawford, 2010; Fiehler, Rösler, & Henriques, 2010; Jones & Henriques,

2010; Khan, Pisella, Vighetto et al., 2005; Medendorp & Crawford, 2002; Pouget, Ducom, Torri, & Bavelier, 2002; Sorrento & Henriques, 2008; Thompson & Henriques, 2009; Van Pelt & Medendorp, 2008), which suggests that world-stationary reach targets are coded and updated in a gaze-centered reference frame. This behavioral inference is supported by neurophysiological recordings and imaging results that demonstrate dynamic updating reach targets in posterior parietal cortex (Batista, Buneo, Snyder, & Andersen, 1999; Medendorp, Goltz, Vilis, & Crawford, 2003).

Given the nature of interception, where future target position(s) and available movement time must be inferred from target motion occurring elsewhere in the visual periphery, one cannot simply expect results and mechanisms similar to those observed for stationary targets (Dessing, Oostwoud Wijdenes, Peper, & Beek, 2009b). Because target motion may not be uniquely coded in gaze-centered coordinates (Melcher & Morrone, 2003; Neppi-Mòdona, Auclair, Sirigu, & Duhamel, 2004), movement plans for interception may be generated in both gaze-centered and gaze-independent reference frames (see also Battaglia-Mayer, Caminiti, Lacquaniti, & Zago, 2003; Blohm & Crawford, 2007). Any error in a pre-saccadic reference frame transformation would result in a pre-saccadic transformation bias. While, as argued above, pre-saccadic representation biases may not be present for stationary targets, they may well be for moving targets (see Brooks & Mather, 2000; Johnston & Wright, 1986; Neppi-Mòdona et al., 2004; Tynan & Sekuler, 1982). During manual interception involving saccadic updating, these additional visuomotor biases would yield errors that depend on the initial gaze position.

The present study examines spatial updating mechanisms during manual interception to address whether (1) pointing errors during an open-loop interception task depend on the target’s retinal eccentricity, and if so, (2) whether these errors depend primarily on the final gaze position at the time of reach, reflecting a dynamic gaze-centered updating process. In our experiment, subjects viewed moving targets that were suddenly occluded and needed to be intercepted after some time. In the *fixation condition*, their gaze was stable throughout the trial, while in the *saccade condition* they shifted gaze with a saccade during target occlusion, prior to the initiation of the interceptive movement (Figure 2). We manipulated initial and final gaze directions as well as the required location of interception. Following the reasoning above, interception errors that depend on the post-saccadic target location relative to gaze should reflect a transformation bias of an updated, gaze-centered spatial representation. As mentioned, any errors based on the target location relative to the initial gaze direction, however, might reflect a pre-saccadic transformation bias, a pre-saccadic representation bias, or a combination of both. We show that interception responses depend on the final and, less consistently, the

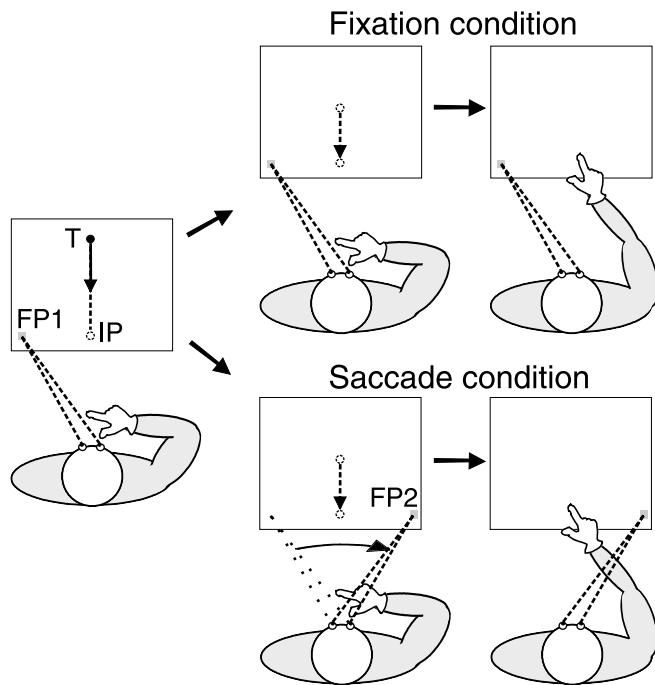


Figure 2. Two conditions used in the saccadic updating paradigm for interception. After fixation at the initial fixation point (FP1), a target (T) appears, which has to be intercepted at fixation height. The ideal interception point (IP) thus must be inferred from target motion in the visual periphery. At some point, the target disappears, which is followed by a memory period. In the *fixation condition*, subjects keep gazing in the same direction in this period, while in the *saccade condition* they shift their gaze using a saccade to the final fixation point (FP2). After the memory period, subjects execute their manual interception movement.

initial retinal target eccentricity. Our analyses suggest that these effects reflect pre-saccadic representation biases and post-saccadic transformation biases.

Methods

Subjects

We tested nine subjects (6 males, 3 females; mean age 25 ± 5 years), who all signed informed consent before participating in the experiment, in line with guidelines of the Institutional Ethics Committee (Commissie Mensgebonden Onderzoek [Committee on Research Involving Human Subjects], Region Arnhem-Nijmegen, The Netherlands). All subjects had normal or corrected-to-normal vision, were right-handed (average laterality quotients: 0.94 [range 0.72–1.00]; Oldfield, 1971), and did not have any known perceptual or motor disorders. They were offered a small fee for their participation (10 euros/h).

Experimental setup

Subjects were seated in a completely darkened room, with their torso strapped into a chair using two safety belts crossing the chest and waist. A chin rest and head band mechanically stabilized the head; their positions were adjusted to individual characteristics. During the experiment, subjects could only move their eyes and right arm and hand, while the rest of the body remained stationary.

An Optotrak Certus System (Northern Digital, Waterloo, Ontario, Canada) measured the 3D position of the fingertip (200 Hz). The actual position of each eye in our setup, defined as its rotation centers, was taken 1.3 cm behind the measured pupil position. The position of the cyclopean eye was computed as the average of the two eye positions. Binocular eye orientations were recorded using an Eyelink II System (SR Research, Mississauga, Ontario, Canada), which was attached to the helmet. The raw pixel coordinates of the pupil centers on the Eyelink images (250 Hz) were used to check fixation online. Trials with erroneous eye movements (e.g., wrong timing/direction of saccade) were repeated at the end of the experiment. Eye movements were calibrated at the start and halfway through the experiment. To this end, pixels were mapped to angles using a regression model (Beurze et al., 2006; Van Pelt & Medendorp, 2007, 2008), calibrated using five horizontal \times four vertical reference positions. Calibration accuracy for the azimuth angle was always $<1^\circ$ (mean of 0.35° across subjects).

All visual stimuli were presented on a 21-inch flat CRT screen (Iyama Vision Master 510, refresh rate of 85 Hz, displaying 1600×1200 pixels). The screen was positioned at a fixed height; its center was 4 cm above and 52 cm in front of the cyclopean eye, implying that the screen on average spanned horizontal and vertical visual angles of -21° to 21° and -20° to 12° , respectively. Brightness settings were adjusted to exclude background light emission (background luminance of the screen was <0.001 cd/m²). A red square of 14×14 pixels ($0.4^\circ \times 0.4^\circ$) served as fixation point (FP), which always appeared 160 pixels (4.0°), from the bottom of the screen (see later for definition of the horizontal position). The target was a red circle with a diameter of 24 pixels (0.7° ; intensity of both FP and target <0.05 cd/m²). A mold, fixed to the chair, positioned about 18 cm in front of the center and 11 cm below the bottom edge of the screen, defined the starting position of the right index finger.

Main paradigm

A trial started (i.e., the FP appeared) when the finger position had remained within 2 cm of the predefined starting position for more than 470 ms. As illustrated in Figure 3A, a white horizontal reference line was shown 1000 ms later for 500 ms, indicating the required height of

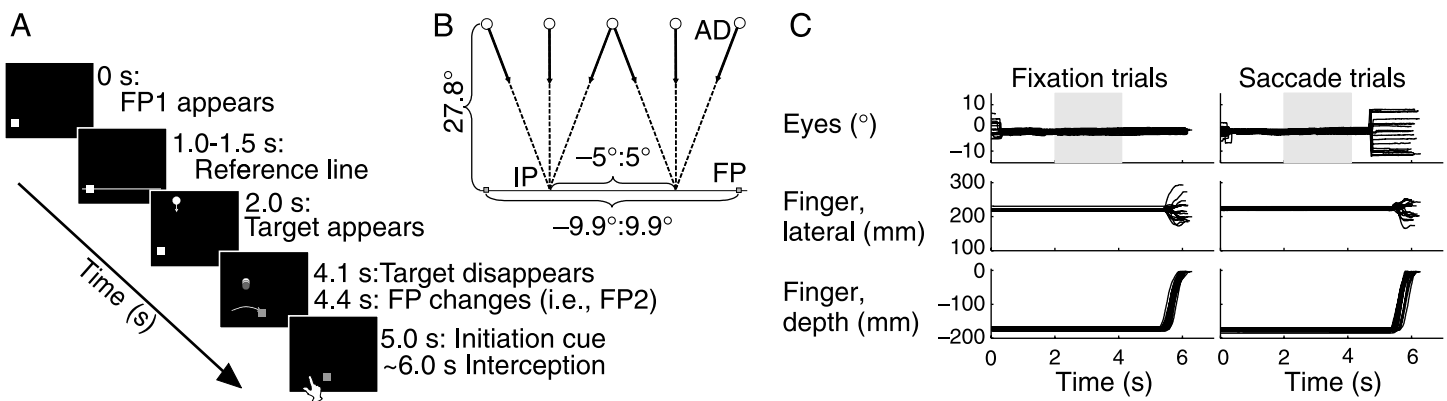


Figure 3. Experimental manipulations. (A) Trial sequence of the experiment. After the initial fixation point (FP1) appeared, a reference line (at fixation height) shortly flashes. Subsequently, the moving target is in view for 2.1 s, after which the location of the fixation point changes (to FP2) in half of the trials (*saccade condition*). Then, an auditory cue signals that the interceptive pointing movement can be initiated (ideally resulting in interception when the target passes fixation height). See text for exact timings. (B) Schematic illustration of the range of target trajectories (as defined by the interception point, IP (most eccentric options shown), and approach direction AD) and fixation points (FPs, both initial and final; most eccentric options shown) used in the experiment. (C) Gaze angles (upper panels) and horizontal (middle panels) and forward finger positions (bottom panels) of a typical subject in *fixation* and *saccade conditions* (left and right panels, respectively). In these trials, the initial fixation was close to straight ahead ($\pm 0.3^\circ$) and the traces are shown until 100 ms after the finger touched the screen. Targets were visible in the gray window indicated for the gaze angles. An auditory initiation cue was presented 5.0 s after trial onset; the target passed fixation height a second later.

interception (which was always the same as fixation height). On each trial, the left and right endings of this line were randomly selected to be 30–150 pixels (0.7° – 4.5°) from the edges of the screen; this was done to prevent target motion to be represented relative to the (edges of the) memorized line. Then, 500 ms later (i.e., 2000 ms after trial onset), a target appeared at the top of the screen (20 pixels or 0.5° from the upper edge), moving down at 3 pixels per frame ($7.1^\circ/\text{s}$) in vertical direction and/or -1 , 0 , or 1 pixel per frame in horizontal direction ($2.4^\circ/\text{s}$, i.e., there were three approach directions, or ADs, see Figure 3B). The horizontal position at which the target passed fixation height (i.e., the interception point, IP) varied quasi-randomly between trials (see below). After the target was shown for 2094 ms, it was rendered invisible (i.e., 554 pixels [15.3°] beneath the upper edge of the screen) followed 294 ms later by a change of the FP (for the *saccade condition*). Subjects were instructed to make a saccade to the new FP as soon as possible following this change. An auditory cue (50 ms) sounded 612 ms later (i.e., 3000 ms after target appearance) to signal that the interceptive movement could be initiated. Subjects were instructed to act as if the invisible target continued to move, intercepting it by touching the screen with their right index finger when and where they thought the target would reach its final position, at fixation height (1000 ms after the auditory cue). In total, invisible target motion thus lasted 1906 ms. Timing requirements did not vary to emphasize the required spatial control, which likely is separate at least to some degree from temporal control (Dessing et al., 2005). Finally, subjects moved their finger back to the starting position, waiting for the

next trial. Subjects never received feedback about their performance.

In our design, the horizontal position of the target trajectories varied as a function of variations in the IP. The horizontal position of IP varied quasi-randomly from 620 to 980 pixels relative to the left edge of the screen (corresponding to -5.0° to 5.0° ; Figure 2B), while the AD was rightward, downward, or leftward. The target thus appeared, disappeared, and passed fixation height at a different position on each trial. IPs were selected from discrete levels with additional random variation in order to reduce the predictability of the experimental conditions. To this end, the employed IP range was divided in four equal bins within which the exact value of IP could be randomly assigned. A similar procedure was used for the quasi-randomization of the initial and final FPs (FP1 and FP2; range of 440–1160 pixels relative to the left edge of the screen, which was -9.9° to 9.9° of visual angle; Figure 2B). With respect to the FPs, our design was build on quartets of trials, comprising all possible combinations of *fixation* and *saccade conditions* given two FPs (i.e., for any FP_A and FP_B , there were fixation conditions at FP_A or FP_B and saccade conditions with gaze shifts from FP_A to FP_B , and vice versa). Because the combinations $\text{FP}_A = \text{FP}_B$ and $\text{FP}_B > \text{FP}_A$ were contained within the quartet of trials, a full range of FP1/FP2 combinations could be generated by only selecting quartets for $\text{FP}_B < \text{FP}_A$. Given four bins for both FP1 and FP2, this yields six bin combinations for which four FP1/FP2 pairs were selected (i.e., six quartets). The resulting 24 FP1/FP2 combinations were run for four IP bins and three ADs, yielding a total of 288 trials in the experiment. In the experiment, these were

presented in fully randomized order. Each trial lasted 7 to 8 s; after 7 trials, the light was turned on for ~5 s to prevent dark adaptation. After 49 trials, a 2-min break was given; each third break involved a recalibration of the eye tracker. Running the experiment took about 90 min.

Control experiment

Six of our subjects were also tested in a control experiment to determine their performance for memorized stationary visual targets in our setup. Stationary targets were presented at the IP positions used in the main experiment (although we selected these positions and FP1 and FP2 positions anew, using the procedure described above). Because there is no AD for stationary targets, the control experiments involved only $288/3 = 96$ trials. The temporal sequence of FP1, reference line, target, FP2 (in the case of the *saccade condition*), auditory cue presentation, and breaks was identical to those in the main experiment. The results of this experiment were generally consistent with earlier findings (Henriques et al., 1998; Medendorp & Crawford, 2002; Van Pelt & Medendorp, 2008) and are therefore only reported in detail in the [Supplementary material](#).

Data analyses

Behavioral characteristics

Data were analyzed offline using Matlab (The Mathworks, Natick, MA, USA). Kinematic data were represented in a Cartesian coordinate frame (origin at the bottom left corner of the screen with the positive *x*-axis pointing rightward, the positive *y*-axis forward, and the positive *z*-axis upward, all from the perspective of the subject). In each trial, movement initiation was defined as the time when the absolute fingertip velocity exceeded 5% of peak velocity. We defined that the finger position touched the screen when the fingertip was less than 1.2 cm from the screen and had a speed lower than 5 mm/s. It may be safely assumed that in our task subjects predict the IP as the movement goal while the target is in view (unlike in other tasks; cf. Dessing et al., 2005; McBeath, Shaffer, & Kaiser, 1995; Peper, Bootsma, Mestre, & Bakker, 1994). Therefore, interception errors were defined as the position where the finger touched the screen relative to the position of the actual IP. While our analyses focused on the horizontal interception errors and timing errors, we also analyzed vertical interception errors and timing errors, because these might indirectly influence horizontal interception errors (i.e., horizontal target position varies with target height/time for oblique trajectories). However, in the [Results](#) section, we show that our observations are not due to such indirect influences.

We evaluated all trials offline for adequate eye and hand movements. We defined gaze direction relative to

the cyclopean eye (see [Figure 3C](#), top panels) and included trial-by-trial drift correction on the basis of the most stable gaze direction (within an interval of 30 consecutive samples) during the last 500 ms before target onset. We included trials if the initial and final gaze were within $\pm 1.5^\circ$ of the required direction. For each trial, we also evaluated whether movements were initiated too early (taking 100 ms after the initiation cue as the earliest allowed initiation). On the basis of these criteria, we excluded 4% of trials (ranging from 0% to 9% across subjects).

Saccade vs. fixation conditions

To quantify the effects of the initial and final IP eccentricities, we fitted the interception errors for each subject using a multiple linear regression model of the form

$$\text{Error} = a + b\text{AD} + c(\text{IP} - \text{FP1}) + d(\text{IP} - \text{FP2}). \quad (1)$$

Here, IP, FP1, and FP2 represent the locations of the interception point and initial and final fixation directions (all expressed in visual degrees relative to the center of the screen), respectively, while AD is the horizontal visual angle between the initial target position and IP. The intercept *a* captures general biases in the interception errors. Pre-saccadic and post-saccadic transformation biases would be reflected in the regression coefficients for (IP – FP1) and (IP – FP2), respectively. Assuming that neural representations of visual targets are renewed as long as visual information is available, representation biases should depend on the most recent available visual conditions. Thus, any effect of retinal eccentricity on the target representation should relate to the eccentricity of the last visible target position, not of the IP. Given that the target was always presented when subjects gazed at FP1, this effect corresponds to the initial eccentricity; representation biases in our task are thus always pre-saccadic. The last visible target position in our task was $\text{IP} - \delta\text{AD}$ (with δ being the proportion of time the target is invisible in our task: $1.9 / 4 = 0.475$). We separated the associated initial eccentricity term (i.e., $\text{IP} - \delta\text{AD} - \text{FP1}$) into contributions of IP eccentricity (IP – FP1) and approach direction (δAD). This analysis was motivated by the possibility of separate effects of AD (Brouwer, Middelburg, Smeets, & Brenner, 2003; Dessing et al., 2005) and (IP – FP1) (see above) on the interception errors. The term (IP – FP1) in our regression model thus captures influences of pre-saccadic representation and/or transformation biases on the interception errors; we devised a new analysis to distinguish between the effects of these biases (see below).

We tested the significance of the unique contribution of each term in the regression models at the single-subject level using *F*-tests ($P < 0.0125$, i.e., Bonferroni corrected for four tests within each subject); these tests evaluate the

variance explained by each factor (i.e., the part not correlated with other factors). It should be noted that for half of the data the terms $(IP - FP_1)$ and $(IP - FP_2)$ were actually identical (i.e., for the *fixation conditions*, $FP_1 = FP_2$). This was not the case in additional regression models, which were applied separately to the *fixation* and *saccade conditions*. The regression coefficients of these separate models were compared using paired-samples *t*-tests.

By definition, these regression analyses assume a linear relationship between the error and the explanatory variables. Because this may not necessarily hold up, we also compared the interception errors between *fixation* and *saccade conditions*, using a trial-by-trial comparison, similar to Beurze et al. (2006). We used the quartets of trials on which we based our design (i.e., all possible combinations between two FPs, yielding four trials: two *fixation* trials at FP_A and FP_B and two *saccade* trials with $FP_A \rightarrow FP_B$ and $FP_B \rightarrow FP_A$). We compared the interception errors between the *fixation* and *saccade* trials with similar initial fixation direction and between those trials with similar final fixation direction. If the interception errors mainly depend on the initial fixation direction, there should be a strong relationship for the first comparison across all trials. Conversely, if they mainly depend on the final fixation direction, there should be a strong relationship for the second comparison across all trials. We assessed the relative contribution of the initial and final fixation directions by comparing the Fisher *Z*-transformed correlation coefficients (*R* values) of the relationships for trial pairs differing in FP_2 and FP_1 , respectively (paired-samples *t*-test; $P < 0.05$).

Representation vs. transformation biases

As pointed out in the [Introduction](#) section, effects of initial eccentricity of the IP relative to gaze may arise in our task due to pre-saccadic representation and/or transformation biases. If our analyses reveal combined effects of initial and final eccentricities, additional analyses are needed to differentiate between these pre-saccadic visuo-motor biases. The first possibility we considered is that initial and final eccentricity effects reflect pre- and post-saccadic transformation biases, respectively. If the IP is stored in separate gaze- and body-centered reference frames, then a transformation into body-centered coordinates occurs both before and after the saccade. The final movement plan must therefore reflect a weighted average of the pre- and post-saccadic movement plans. We applied this to the quartets of trials that defined our experimental design (see previous paragraph). The interception error in a *saccade* trial ($FP_A \rightarrow FP_B$) should thus reflect a weighted average of the transformation biases for FP_A and FP_B (i.e., $\beta T_A + (1 - \beta)T_B$, with subscripts “A” and “B” referring to the FPs and $0 < \beta < 1$), while in a *fixation* trial (for FP_A or FP_B) it should reflect just one transformation bias (T_A or

T_B). It follows that the interception error in the *saccade* trial should be predictable from the weighted average of the interception errors in the corresponding *fixation* trials (i.e., $\beta \text{Error}_{FP_A} + (1 - \beta) \text{Error}_{FP_B}$). We assessed this prediction across all trials using the associated Fisher *Z*-transformed *R* values, which we compared across subjects with those from the original single-trial relationships ($P < 0.025$, i.e., Bonferroni corrected for two comparisons). While in the text we mainly present the outcome for an equal weighting of the gaze- and body-centered plans (i.e., $\beta = 0.5$), we confirmed our conclusions for the entire range of relative weightings.

A second possibility is that effects of initial and final eccentricities reflect pre-saccadic representation biases and post-saccadic transformation biases, respectively. One *saccade* trial of the quartet ($FP_A \rightarrow FP_B$) would reflect a pre-saccade representation bias R_A and a post-saccadic transformation bias T_B , while the other *saccade* trial ($FP_B \rightarrow FP_A$) would reflect R_B and T_A . Similar biases in the corresponding *fixation* trials (FP_A , FP_B) would yield R_A and T_A , and R_B and T_B , respectively. Thus, if interception performance reflects pre-saccadic representation and post-saccadic transformation biases, the summed interception errors of the two *fixation* trials in each quartet should be predictable from those of the two *saccade* trials. We assessed this prediction across all trials using the associated Fisher *Z*-transformed *R* values, which we compared across subjects with those of all three of the aforementioned relationships ($P < 0.017$, i.e., Bonferroni corrected for three comparisons).¹

Results

This study was designed to explore the effects of gaze direction and intervening saccades on manual interception movements. In our task, the goal had to be inferred from an extinguished target that was previously moving elsewhere in the visual periphery. Our analyses specifically focus on the difference between our *fixation condition* (involving stable fixation during the entire trial) and our *saccade condition* (involving a gaze shift just after target occlusion; see [Figure 2](#)), in order to provide insights into the reference frames underlying the representation of the spatial goal for manual interception.

For comparison, subjects also made reaching movements to stationary targets, with and without intervening saccades. The results of this control experiment replicated many previous studies (e.g., Henriques et al., 1998; Sorrento & Henriques, 2008; Van Pelt & Medendorp, 2008): The reach errors were predominantly affected by the target’s eccentricity just before reach onset (see [Supplementary material](#)). These findings suggest that a gaze-centered representation of the stationary target is

updated across the saccade and only subsequently transformed into body-centered coordinates. The question is: are similar mechanisms involved in manual interception?

Figure 4 illustrates the range of observed interception movements in both *fixation* and *saccade conditions*, as a function of the initial and final eccentricities of the IP. We calculated the average biases in the finger movements in the transversal plane, relative to straight line from the initial finger position to the IP (Figure 4A). These averages were determined separately for trials with the

FP to the left and right of the IP; because the *saccade* trials contain two FPs, two separate averages were calculated for this condition. For reference, Figure 4B shows how pure effects of initial and final eccentricities would impact the movement biases. Importantly, the shape and direction of the predicted trajectories is arbitrary; the prediction only concerns the pattern in the difference between positive and negative IP eccentricities across the *fixation* and *saccade conditions*. If the interception movements only depend on the initial (final)

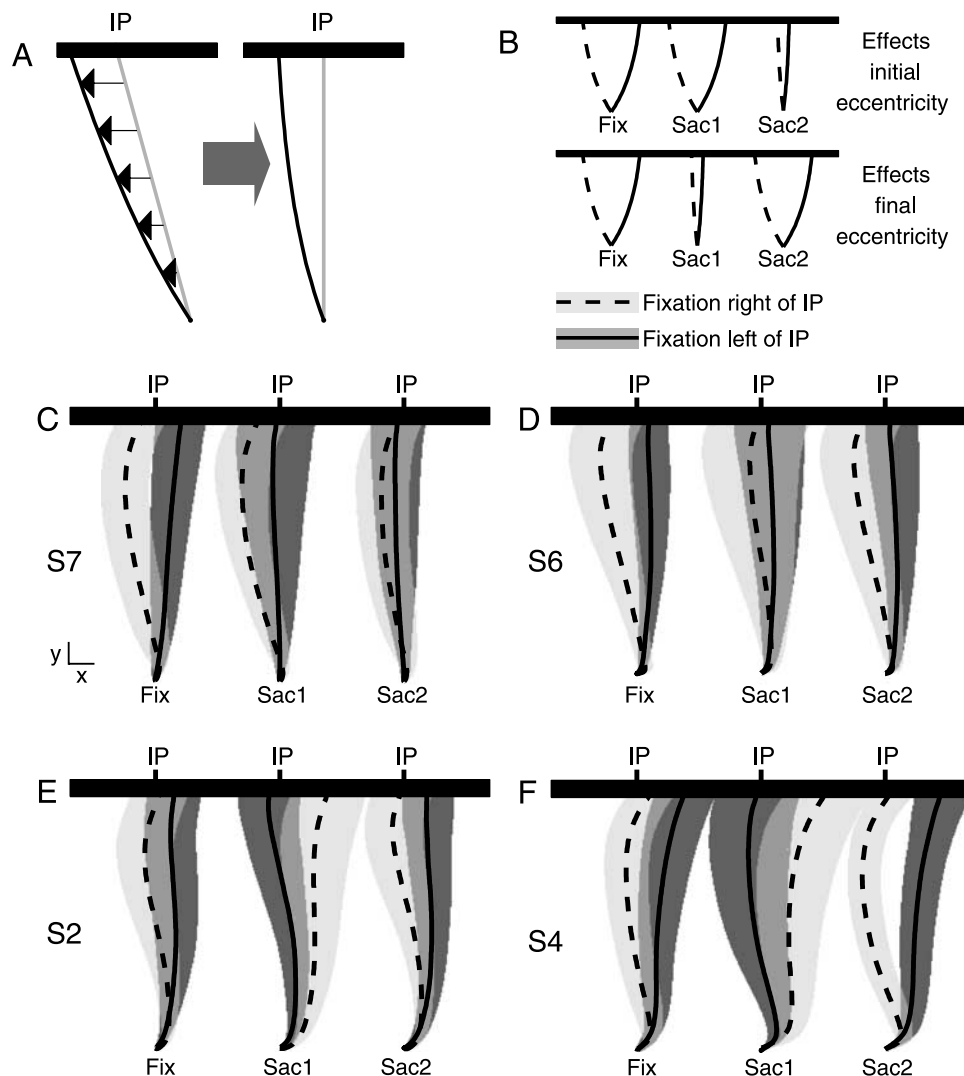


Figure 4. Illustration of movement biases. (A) Method to calculate biases in the movement trajectories. The trajectories of all trials were expressed relative to a straight line from the initial finger position and interception point (IP) before being averaged (illustrated for several arbitrary points along the trajectory using arrows). To better illustrate the effects, we calculated separate averages for trials with the FP to the left of the IP and those with the FP to the right of the IP. For the *fixation condition* (fix), this referred to FP1; for the *saccade condition*, this averaging was done twice, once referring to FP1 (sac1) and once referring to FP2 (sac2). For illustrative purposes, only trials with more eccentric IPs ($IP - FP < -5^\circ$ / $IP - FP > 5^\circ$) were used. (B) Predicted initial and final eccentricity-dependent movement biases for the *fixation condition* and for the *saccade condition*. These predictions refer to the pattern across fix, sac1, and sac2, not to the specific shape of movement bias curves. (C–F) Average top view of the biases in the finger movements and their 95% confidence intervals of four subjects; different grayscales and line types are used for trials with the FP (i.e., that used to calculate the average movement biases) to the left and right of the IP. Where the 95% confidence intervals overlap, an intermediate grayscale is used. The axes in (C) correspond to 2 cm.

| Subject | <i>a</i> | <i>b</i> | <i>c</i> | <i>d</i> | <i>R</i> |
|---------|--------------|--------------|--------------|--------------|-------------|
| 1 | 0.75 | 0.20 | −0.01 | −0.10 | 0.61 |
| 2 | −1.78 | 0.13 | −0.15 | 0.15 | 0.63 |
| 3 | −2.54 | 0.12 | 0.09 | −0.08 | 0.39 |
| 4 | −0.51 | 0.02 | −0.21 | 0.27 | 0.57 |
| 5 | −0.04 | 0.08 | −0.16 | −0.08 | 0.64 |
| 6 | −2.06 | 0.15 | 0.02 | 0.13 | 0.58 |
| 7 | −3.13 | −0.03 | 0.11 | 0.05 | 0.41 |
| 8 | −2.78 | 0.11 | 0.00 | 0.16 | 0.49 |
| 9 | −5.66 | −0.04 | −0.12 | 0.16 | 0.45 |

Table 1. Gaze-centered effects in interception. *Note:* *Fitting Error = $a + bAD + c(IP - FP1) + d(IP - FP2)$ to the horizontal interception errors of each subject. Significant regression coefficients (first four columns) and correlation coefficients (*R*, last column) are depicted in boldface.

eccentricity, the effect of eccentricity in the *fixation condition* should match the effect calculated with FP1 (FP2) for the *saccade condition*, while there should be no difference between final (initial) fixation left and right of the IP (i.e., the lines for sac2 (sac1) should overlap). If there are combined effects of initial and final eccentricities, there should be an effect of fixation direction for both sac1 and sac2.

Figures 4C–4F show the movement biases ($\pm 95\%$ confidence interval) for four subjects throughout the reach, which proved not to uniquely reflect only the initial or final eccentricity. One subject primarily showed effects of initial IP eccentricity (Figure 4C) and another mainly of the final IP eccentricity (Figure 4D). The movement biases of two other subjects did not match either of the predictions of Figure 4B. One of these appeared to show effects of final eccentricity in the *fixation condition*, with additional effects of initial eccentricity in opposite direction in the *saccade condition* (Figure 4E). For the other subject, the smaller effects in the *fixation condition* appeared to be the sum of the opposite effects of initial and final eccentricities in the *saccade condition* (Figure 4F). Both these subjects thus showed movement biases that depended on both the initial and final IP eccentricities. A

pattern suggestive of such combined effects was common across our subjects. It is important to realize that these movement biases are only illustrative, because they have been calculated using a subset of trials and detailed effects of eccentricity have been averaged out. Nevertheless, our statistical analyses of endpoint biases (i.e., the interception errors) largely confirmed the patterns discussed above, as will be shown next.

Model analysis of horizontal interception errors

We analyzed the interception errors using a multiple linear regression model. Since the variability of the interception errors did not vary significantly with approach direction (single-subject Levene's tests, all $P > 0.12$; Brouwer et al., 2003), data from all three approach directions were included in a single regression model. For each subject, we fit the horizontal interception errors using Error = $a + bAD + c(IP - FP1) + d(IP - FP2)$. All fits were significant ($P < 10^{-8}$ for all subjects), with *R* values ($0.39 < R < 0.65$) comparable to previous studies involving stationary targets (Beurze et al., 2006; Van Pelt & Medendorp, 2008). Table 1 lists the coefficients for the regression models, demonstrating that the interception errors depended on the final eccentricity in all subjects but one (Subject 7). This pattern suggests a dominance of gaze-centered transformation biases, consistent with previous observations for stationary targets (Henriques et al., 1998; Medendorp & Crawford, 2002; Sorrento & Henriques, 2008; Van Pelt & Medendorp, 2008). Furthermore, in six subjects, there was an effect of initial eccentricity; five of these actually showed both effects. As described in the Introduction section, effects of initial eccentricity suggest the presence of pre-saccadic representation or transformation biases.

To further compare the *fixation* and *saccade conditions*, we also modeled the interception errors of these conditions separately (see Table 2, subscripts “fix” and “sac” used to distinguish the regression coefficients of the

| Subject | <i>a</i> _{fix} | <i>a</i> _{sac} | <i>b</i> _{fix} | <i>b</i> _{sac} | <i>c</i> _{fix} | <i>c</i> _{sac} | <i>d</i> _{sac} | <i>R</i> _{fix} | <i>R</i> _{sac} |
|---------|-------------------------|-------------------------|-------------------------|-------------------------|-------------------------|-------------------------|-------------------------|-------------------------|-------------------------|
| 1 | 0.62 | 0.84 | 0.17 | 0.22 | −0.09 | −0.03 | −0.13 | 0.54 | 0.68 |
| 2 | −1.84 | −1.68 | 0.11 | 0.15 | 0.06 | −0.23 | 0.08 | 0.52 | 0.75 |
| 3 | −2.37 | −2.74 | 0.08 | 0.15 | 0.07 | 0.03 | −0.13 | 0.27 | 0.55 |
| 4 | −0.63 | −0.39 | 0.02 | 0.02 | 0.13 | −0.27 | 0.20 | 0.36 | 0.70 |
| 5 | −0.14 | 0.07 | 0.04 | 0.12 | −0.26 | −0.15 | −0.07 | 0.70 | 0.61 |
| 6 | −2.22 | −1.91 | 0.13 | 0.17 | 0.16 | 0.01 | 0.11 | 0.63 | 0.56 |
| 7 | −2.96 | −3.33 | −0.04 | −0.02 | 0.17 | 0.10 | 0.04 | 0.48 | 0.31 |
| 8 | −2.74 | −2.78 | 0.08 | 0.15 | 0.18 | −0.02 | 0.14 | 0.51 | 0.51 |
| 9 | −5.72 | −5.61 | −0.08 | −0.01 | 0.05 | −0.13 | 0.15 | 0.36 | 0.53 |

Table 2. Separate fits to the data in the fixation and saccade conditions. *Note:* *Fitting Error_{fix} = $a_{fix} + b_{fix}AD + c_{fix}(IP - FP1)$ to the interception errors in the *fixation condition* and Error_{sac} = $a_{sac} + b_{sac}AD + c_{sac}(IP - FP1) + d_{sac}(IP - FP2)$ to those in the *saccade condition* for each subject. Significant regression coefficients (first seven columns) and correlation coefficients (*R*_{fix} and *R*_{sac}) are depicted in boldface.

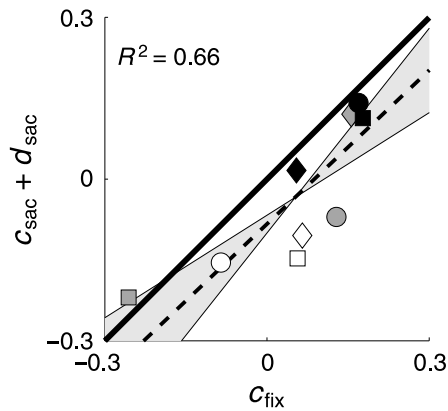


Figure 5. Combined effects of initial and final eccentricities: regression coefficients. Relationship between the regression coefficients related to the eccentricity of the interception point (IP – FP) in the *fixation condition* (c_{fix}) and the summed regression coefficients related to the initial and final eccentricities of the interception point (IP – FP1 and IP – FP2) in the *saccade condition* ($c_{\text{sac}} + d_{\text{sac}}$). The figure also shows the unity line (thick black line), the best fitting relationship (dashed line, as determined using model II regression, York, 1966), and the 95% confidence intervals of the slopes (gray area). Different subjects are indicated by different symbols, used consistently throughout this paper. (○:S1, □:S2, ◇:S3, ●:S4, ■:S5, ◆:S6, ●:S7, ■:S8, ◆:S9).

fixation and *saccade conditions*, respectively). Note that, by design, for the *saccade conditions* factors (IP – FP1 and IP – FP2) were uncorrelated for all subjects ($-0.08 < R < 0.06$; all $P > 0.32$). *F*-tests of the different factors revealed that five of our subjects showed a significant gaze-centered overshoot in the *fixation condition* (i.e., significantly positive c_{fix} in Table 2; in two subjects, the effect failed to reach significance), as observed before for stationary targets (Beurze et al., 2006; Bock, 1986; Enright, 1995; Henriques et al., 1998). The remaining two subjects showed a significant gaze-centered undershoot. In the *saccade condition*, these two plus an additional subject also showed a significant undershoot relative to final gaze position. For one subject (S5), these undershoots reflected the behavior for stationary targets (Supplementary material); for the others, these undershoots may reflect differences in the visuomotor transformation for stationary and moving targets.

We used these regression models to further examine the effects of eccentricity independently of their specific direction within subjects (for a similar methodology, see Beurze et al., 2006; Scherberger, Goodale, & Andersen, 2003; Van Pelt & Medendorp, 2008). If both effects play a role, the weight of the eccentricity-dependent effect in the *fixation condition* should reflect a combination of the initial and final eccentricity effects in the *saccade condition*. Specifically, if these effects have different origins, they should sum. Across subjects, this prediction was confirmed qualitatively in that the explained variance

of the relationships between c_{fix} and c_{sac} and between c_{fix} and d_{sac} across subjects was only 7% and 38%, respectively, while it was 66% for the relationship between c_{fix} and $c_{\text{sac}} + d_{\text{sac}}$ (see Figure 5).² The slope of the latter relationship (0.95) was not significantly different from unity.

Comparison of interception errors between fixation and saccade conditions

We sought to support the mixed effects using an analysis not relying on the assumption of linearity implicit to any regression model. We first applied an established analysis to capture the *relative* strengths of the effects of initial or final eccentricity, again independently of the direction and size of the effects for individual subjects (e.g., Beurze et al., 2006). This comparison involved trials from the quartets of trials (i.e., all possible *fixation* and *saccade* trials given two FPs; see Methods section for detailed explanation). If the interception errors mainly depend on the initial fixation direction, there should be a strong relationship between the errors in *fixation* and *saccade* trials with similar initial fixation direction. Conversely, if they mainly depend on the final fixation direction, there should be a strong relationship between the errors in *fixation* and *saccade* trials with similar final fixation direction. We assessed the relative contribution of the initial and final fixation directions by comparing the *R* values for these relationships. Figure 6 depicts both relationships for two subjects, the one subject showing a higher *R* for the relationship based on trial pairs with the same final eccentricity (Figures 6A and 6B) and the other showing a higher *R* for the relationship based on trial pairs with the same initial eccentricity (Figures 6C and 6D).

Before comparing these *R* values across subjects, we confirmed that the slopes for both relationships were not significantly different from 1 (Student's *t*-tests, $P > 0.21$). As depicted in Figure 6E, the *R* values clearly were rather low and varied considerably across subjects. They were not significantly different between the relationships ($t(8) = 0.42$; $P > 0.68$). Consistent with the regression models, this analysis thus suggested that the influence of neither the initial nor final IP eccentricity was clearly dominant. This, however, would be expected if interception errors reflect mixed influences of both eccentricities.

We therefore extended this analysis to test whether an explanation in terms of mixed influences of initial and final eccentricities provides a statistically better account of the observed interception errors. As outlined in the Introduction section and Methods section, the combined effect of initial and final eccentricities on the interception error could reflect pre- and post-saccadic transformation biases, which would arise if movement plans are generated in parallel in gaze- and body-centered coordinates. As explained in the Methods section, this hypothesis

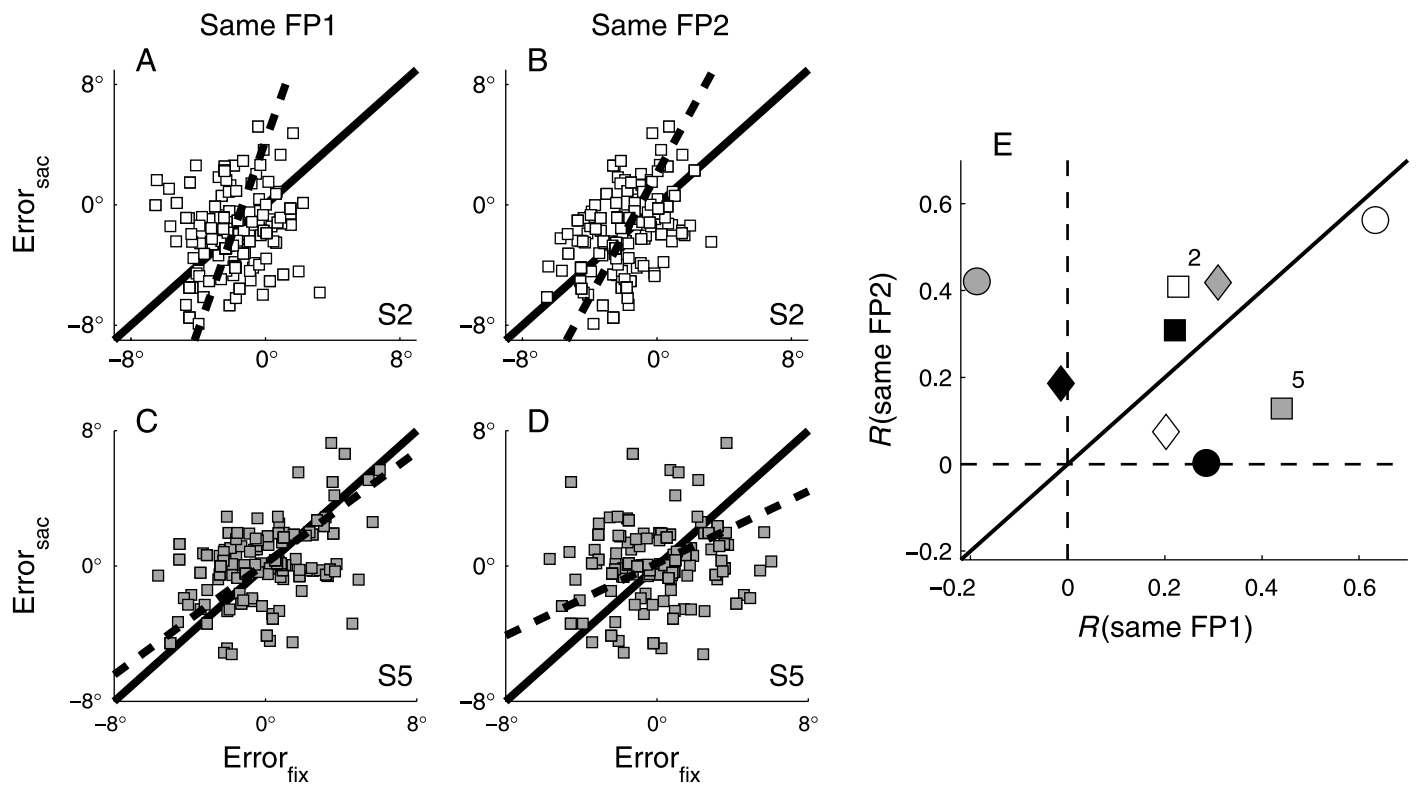


Figure 6. Single-trial interception errors. For two subjects, from a quartet of trials, we depict interception errors in *fixation* and *saccade* conditions with similar FP1s (A and C) and those with similar FP2s (B and D). Each panel also shows a unity line (thick black line) for reference, while the best fitting line (York, 1966) is presented in (A) to (D) (dashed line). (E) The correlation coefficient obtained in both relationships for all subjects ($R(\text{same FP1})$ and $R(\text{same FP2})$).

predicts that the interception error in a *saccade* trial should be similar to the weighted average of the interception errors of two *fixation* trials involving the same FPs. Across subjects, however, the slopes of this relationship for all trials differed significantly from 1 for a large range of relative weightings used for the weighted average ($0.03 < \beta < 0.61$; see [Methods](#) section). Moreover, the R values of the relationship were not significantly higher than both R values of the relationships for similar FP1s and FP2s for any value of β . This implies that, across subjects, the hypothesis of combined pre- and post-saccadic transformation biases does not provide a significantly better account of our data than the original hypotheses of pure pre- or post-saccadic transformation biases.

Therefore, we tested whether the observed interception errors reflected combined pre-saccadic representation biases (i.e., biases in target-related, effector-independent signals) and post-saccadic transformation biases. This hypothesis predicts that the sum of the interception errors of two *saccade* trials should be equal to the sum of the interception in the two associated *fixation* trials ($\text{Error}_{\text{FP}_A \rightarrow \text{FP}_B} + \text{Error}_{\text{FP}_B \rightarrow \text{FP}_A} = \text{Error}_{\text{FP}_A} + \text{Error}_{\text{FP}_B}$; see [Methods](#) section). In [Figures 7A](#) and [7B](#), we show the associated relationships across trials for two subjects. Across subjects, the slope of this relationship did not

differ significantly from 1 (Student's t -test; $P > 0.15$). [Figures 7C–7E](#) show that the R values are significantly higher than the R values of all aforementioned relationships (i.e., values above the unity line; t and P values depicted in panels). For the last comparison, this was found to hold irrespective of the value of the relative weighting (β) that was used. Even though the effect of noise increases for summed errors, the R values were comparable in magnitude to previous observations (Beurze et al., 2006; Van Pelt & Medendorp, 2007). Across subjects, the hypothesis of combined representation and transformation biases thus provides the best account of the interception errors observed in our experiment.

Additional influences on interception errors

Our analyses so far assumed that subjects predicted the IP at some position on the indicated reference line. A misrepresentation of the height of the reference line, however, could affect the computation of the predicted IP. The vertical interception errors provide a marker of this computation. In general, our subjects touched the screen below the reference line; in only four subjects, this vertical error depended on the final horizontal eccentricity

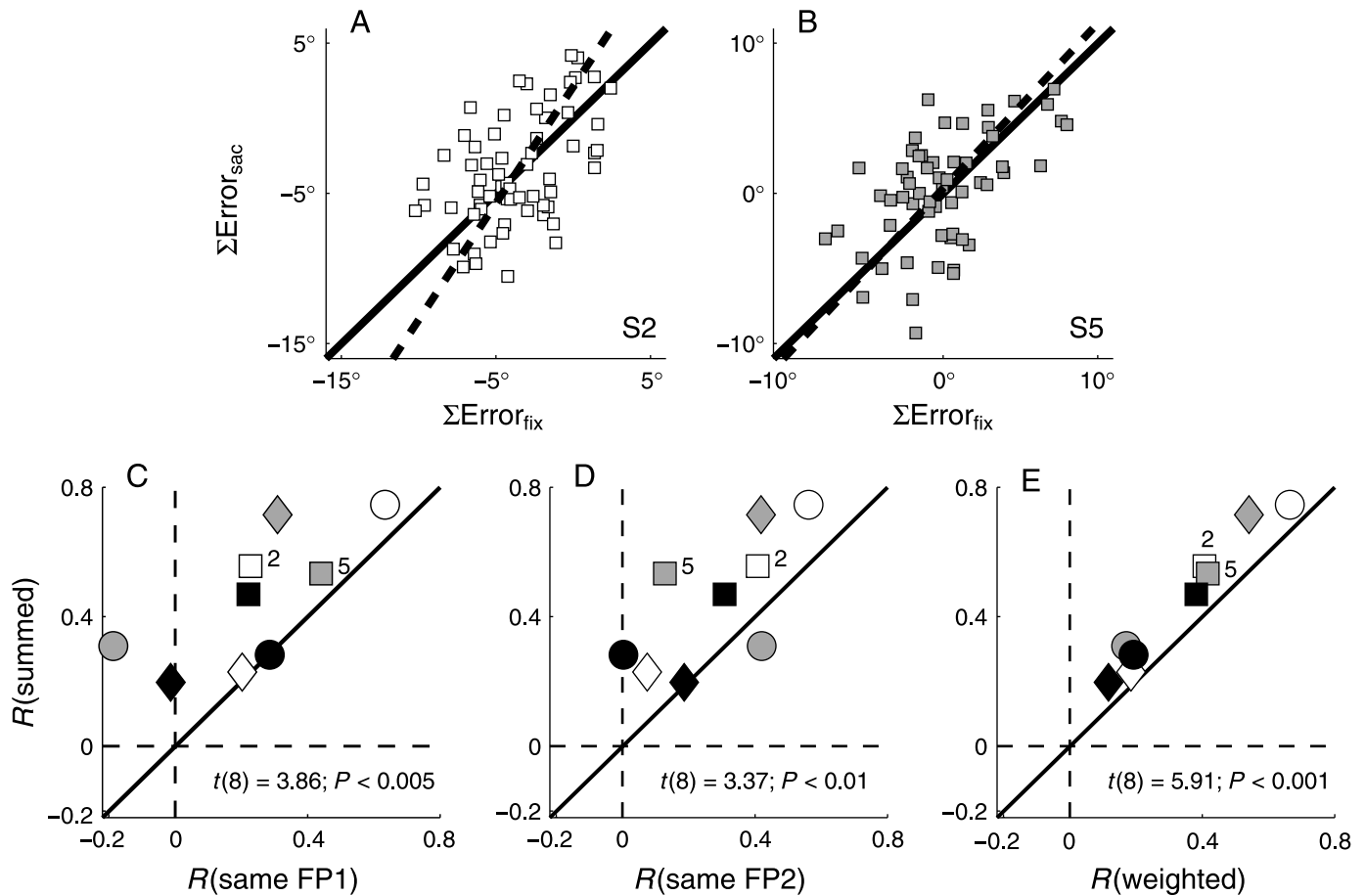


Figure 7. Analysis of summed interception errors specific to combined representation and transformation biases. For two subjects, we depict the summed interception errors for the *saccade condition* ($\Sigma\text{Error}_{\text{sac}}$) as a function of those of the *fixation condition* ($\Sigma\text{Error}_{\text{fix}}$), selected out of a quartet of trials with similar IPs and ADs (A and B). Each panel also shows a unity line (thick black line) for reference, while the best fitting line (York, 1966) is also presented in (A) and (B) (dashed line). (C–E) For all subjects, the resulting correlation coefficients ($R(\text{summed})$) are given as a function of those obtained for the single-trial relationships ($R(\text{same FP1})$ and $R(\text{same FP2})$) and for the relationship based on weighted interception errors ($R(\text{weighted})$; values shown for $\beta = 0.5$).

of the IP (see [Supplementary Table 2](#)). In addition, none of the comparisons of the R values for relations based on single-trial or summed interception errors (i.e., those depicted in [Figures 6](#) and [7](#)) yielded a significant difference (all $P > 0.25$). Similar analyses for the temporal interception errors did not reveal any consistent pattern (the full regression model was significant for only two subjects (see [Supplementary Table 3](#)), while none of the comparisons of R values yielded a significant difference (all $P > 0.39$).

While the effects of final eccentricity for four subjects could artificially induce effects of final eccentricity on their horizontal interception errors, these would be in opposite direction for the two oblique trajectories. However, such opposite effects would not cancel out completely if the vertical interception error at each eccentricity differs in size for those two ADs. We calculated that the asymmetry in our data was so small that it could only account for a marginal part (0.1 degree)

of the observed effect of eccentricity on the horizontal interception errors. We are thus confident that our main findings are not side effects of variations in the interception height.

In addition to the eccentricity effects, our regression models also tested for general biases and effects of target approach direction (AD). It is most informative to describe these effects using the models applied separately to the *fixation* and *saccade conditions*. The intercepts in these models (a_{fix} and a_{sac} ; [Table 2](#)) indicated a minor leftward bias ($\sim 2^\circ$), which did not statistically differ between *fixation* and *saccade conditions* ($P > 0.56$). The AD coefficients were positive on average; because targets were also hit below the reference line, this suggests that targets were hit further along its trajectory. This effect was larger when a saccade was made ($b_{\text{sac}} > b_{\text{fix}}$; $t(8) = 5.13$; $P < 0.001$). For models with the term (IP – 0.475AD – FP1, see [Methods](#) section) instead of (IP – FP1), however, this difference was not significant ($P > 0.71$).

We thus interpret the mentioned difference to be a by-product of the fact that representation biases depend on the last visible target position.

Discussion

In this study, we examined the role of gaze direction during manual interception. We assessed to what extent interception errors depend on the initial and final eccentricities of the interception point relative to gaze in a spatial updating paradigm, in which a saccade is made between viewing and reaching toward a moving target. In a control task involving stationary targets, we replicated the previous findings (i.e., gaze-centered overshoots and updating; Baker, Harper, & Snyder, 2003; Henriques et al., 1998; Medendorp & Crawford, 2002; Poljac & van den Berg, 2003; Pouget et al., 2002; Sorrento & Henriques, 2008; Van Pelt & Medendorp, 2007, 2008; see [Supplementary material](#)). Similar but more variable effects occurred for interception. This variability reflected additional effects of the initial IP eccentricity for some of our subjects. Such effects have not been reported for stationary targets and appear to be unique and specific to manual interception, at least in healthy subjects with intact brains (Khan, Pisella, Rossetti, Vighetto, & Crawford, 2005).

In line with previous studies, we interpret the effect of final eccentricity to reflect a bias in the transformation of the updated representation of the IP into an action-specific body-centered reference frame (Henriques et al., 1998; McGuire & Sabes, 2009; Van Pelt & Medendorp, 2008). Such transformation biases could also explain the findings of Poljac, Neggers, and van den Berg (2006), who reported eccentricity-dependent biases when the prediction impact location of a target approaching the head was manually indicated but not when subjects were asked to verbally report it.

Eccentricity-dependent representation biases in interception

The observed effects of initial eccentricity were shown to reflect representation biases arising in the target-related signals used to compute the movement plan (see also Dessing et al., 2009b). These appear to depend on the retinal eccentricity of the target *when it is in view* (i.e., early during the trial, before the saccade in the *saccade condition*). In [Appendix A](#), we show how the behavioral effects of representation biases remain dependent on the initial eccentricity even after a saccade, that is, after gaze-centered updating.

The general absence of effects of initial eccentricity in our control experiment with stationary targets suggests

that these representation biases somehow arise specifically when the sensory input includes target motion. Because motion biases may arise as early as the retina (Berry, Brivanlou, Jordan, & Meister, 1999), they may influence performance in tasks that do not involve hand movements (e.g., perceptual tasks). Indeed, previous studies have shown that perceived target motion is influenced by retinal eccentricity (Brooks & Mather, 2000; Johnston & Wright, 1986; Neppi-Mòdona et al., 2004; Tynan & Sekuler, 1982). Our data suggest that the magnitude of these target motion-related representation biases varies across subjects (see also Neppi-Mòdona et al., 2004).

Given the existence of distinct neural pathways for the coding of target position and motion (Krauzlis, 2004), different reference frames may be used to code target position and velocity. Gaze-centered mechanisms have been suggested to underlie early visual motion detection (Berry et al., 1999; Morvan & Wexler, 2005; Wenderoth & Wiese, 2008), while later motion detection (i.e., after 130 ms; Morvan & Wexler, 2005) and target velocity memory (Ong, Hooshvar, Zhang, & Bisley, 2009) employ gaze-independent (i.e., spatiotopic) mechanisms. Visual motion signals of 150 ms can indeed be integrated across saccades in gaze-centered as well as gaze-independent reference frames (Melcher & Morrone, 2003). Gaze-centered and head-centered reference frames are also used for extrapolation of target motion (Neppi-Mòdona et al., 2004). In a slightly different paradigm, Harris and Dean (2003) and Welchman, Tuck, and Harris (2004; but see Welchman, Harris, & Brenner, 2009) observed similar biases during fixation and pursuit, suggesting a gaze-independent origin. Finally, allocentric cues such as stationary and moving structured backgrounds (not employed here) may also influence target motion signals (Blakemore & Snowden, 2000; Brenner & Smeets, 1994; Dessing et al., 2005; Smeets & Brenner, 1995; Soechting, Engel, & Flanders, 2001).

At the neurophysiological level, the middle temporal complex (MT+/V5 in humans, MT and MST in monkeys) plays a central role in the coding of target motion, also during manual interception (Bosco, Carrozzo, & Lacquaniti, 2008; Ilg & Schumann, 2007; Schenk, Ellison, Rice, & Milner, 2005; see also Boulinguez, Savazzi, & Marzi, 2009; Senot, Baillet, Renault, & Berthoz, 2008). MT+/V5 has been reported to use a gaze-centered reference frame (Gardner, Merriam, Movshon, & Heeger, 2008; Krekelberg, Kubischik, Hoffmann, & Bremmer, 2003; Pitzalis et al., 2010, but see d'Avossa et al., 2007), although MST appears to employ gaze-independent coding (Ilg, Schumann, & Thier, 2004; Inaba, Shinomoto, Yamane, Takemura, & Kawano, 2007), possibly through gain modulations by eye position signals (Bremmer, Pouget, & Hoffmann, 1998). Signals from MT+/V5 reach a range of parietal motion-sensitive areas, such as area 7a, lateral intraparietal area (LIP), and the superior parietal-occipital cortex (SPOC; see Boussaoud, Ungerleider, & Desimone, 1990; Cavada &

Goldman-Rakic, 1989; Colby, Gattass, Olson, & Gross, 1998; Ungerleider & Desimone, 1986). Area 7a is involved in interception (Merchant, Battaglia-Mayer, & Georgopoulos, 2004) and may use head-centered coding (Siegel, 1998). LIP performs extrapolation of target motion (Assad & Maunsell, 1995; see also Olson, Gatenby, Leung, Skudlarski, & Gore, 2004; Shuwairi, Curtis, & Johnson, 2007) and employs a mixture of gaze-centered and head-centered reference frames (Mullette-Gillman, Cohen, & Groh, 2005, 2009; Stricanne, Andersen, & Mazzoni, 1996). Finally, area SPOC (which may partly include area V6(A); Galletti, Gamberini, Kutz, Baldinotti, & Fattori, 2005) is also involved in reaching and appears to encode peripheral targets in a gaze-centered coordinate frame (Beurze, Toni, Pisella, & Medendorp, 2010; Galletti, Fattori, Kutz, & Gamberini, 1999; Marzocchi, Breveglieri, Galletti, & Fattori, 2008; Vesia, Prime, Yan, Sergio, & Crawford, 2010).

Thus, both psychophysical and neurophysiological studies suggest that target motion signals may be coded in both a gaze-centered frame and a variety of other gaze-independent (e.g., body-centered) reference frames in the brain. We propose that (eccentricity-dependent) representation biases arise in the initial gaze-centered stages, which would explain the effects of initial eccentricity on manual interception responses in some of our subjects.

Additional factors

The aforementioned sections summarized evidence for the existence of both gaze-centered and gaze-independent (i.e., head-, body- or world-centered) representations of target motion. This evidence may, in fact, suggest that movement plans are generated in both gaze- and body-centered reference frames (Dessing, Crawford, & Medendorp, 2010). Indeed, even for stationary targets, studies have suggested a role for gaze-centered reference frames, as well as head-centered (Duhamel, Bremmer, BenHamed, & Graf, 1997; Martinez-Trujillo, Medendorp, Wang, & Crawford, 2004; Park, Schlag-Rey, Schlag, 2006), shoulder-centered (Beurze et al., 2006; Blohm & Crawford, 2007; Khan et al., 2007; see also McGuire & Sabes, 2009), hand-centered (Heuer & Sangals, 1998; Lemay & Stelmach, 2005; McIntyre, Stratta, & Lacquaniti, 1998), and allocentric reference frames (Byrne et al., 2010; Carrozzo, McIntyre, Zago, & Lacquaniti, 1999). This possibility gains some plausibility from the fact that interception is a more complex task than reaching to stationary remembered targets, perhaps requiring the brain to make use of every mechanism at its disposal to simultaneously store and process data. While we showed that additional gaze-independent mechanisms do not explain the effects of initial eccentricity as well as the proposed gaze-centered representation biases, we cannot exclude that a small part of the effect of initial eccentricity may be due to pre-saccadic transformation biases.

If the interception errors were, in fact, influenced by saccade amplitude ($FP2 - FP1$), our regressions models would have also yielded significant terms of the initial and final eccentricities with opposite signs (i.e., $(FP2 - FP1) = (IP - FP1) - (IP - FP2)$). For the *saccade condition*, a regression model with the term $(FP2 - FP1)$ instead of $(IP - FP1)$ and $(IP - FP2)$ explained significantly less variance than the original model ($t(8) = 3.32$; $P < 0.05$). Because this might reflect the lower number of parameters, we also added the term IP . For this model, the R values did not differ statistically from those of the original model (Table 2), while they still did for the *fixation condition* ($t(8) = 2.32$; $P < 0.05$). This supports an explanation based on retinal eccentricity, but it also suggests that future studies should investigate the contributions of these additional factors in more detail. Such studies could also focus on other factors not considered by our analysis, such as effects of the direction of the IP (i.e., adding this factor would make our model overdetermined). These effects may be distinguished using subsets of trials in which only a subset of conditions vary.

Conclusions

Our spatial updating paradigm for manual interception yielded an important new insight that could not be predicted from reaching toward stationary targets: namely, that interceptive reaches are influenced by both the initial and final gaze directions during spatial updating tasks. We interpreted the effect of final eccentricity in terms of biases arising in the transformation of the gaze-centered goal position or movement plan into body-centered coordinates. The effect of initial eccentricity was interpreted to reflect biases in the target-related signals used to calculate the movement plan. Thus, while similar mechanisms may underlie manual interception and reaches to stationary targets, additional biases arise during interception because the target is moving.

Appendix A

The process of gaze-centered updating can be illustrated using a simple, linear, one-dimensional model for a situation with a saccade from FP_A to FP_B . The initial gaze-centered representation of a target (T_{GC}) depends on the position of the target (T) relative to an initial fixation point (FP_A):

$$T_{GC} = (T - FP_A). \quad (A1)$$

The updating process that keeps this representation aligned with gaze direction involves correcting for the saccade amplitude, $(FP_B - FP_A)$:

$$T_{GC} = (T - FP_A) - (FP_B - FP_A) = (T - FP_B). \quad (A2)$$

An eccentricity-dependent transformation bias arises within the transformation to body-centered coordinates, which can be represented by adding the final gaze direction (FP_B) plus an eccentricity-dependent error:

$$T_{BC} = (T - FP_B) + FP_B + b(T - FP_B). \quad (A3)$$

This indeed yields a pointing error (i.e., relative to the target) that depends on the final target eccentricity:

$$\begin{aligned} \text{Error}_{BC} &= (T - FP_B) + FP_B + b(T - FP_B) - T \\ &= b(T - FP_B). \end{aligned} \quad (A4)$$

Effects of the final eccentricity during manual interception may be explained by a similar mechanism. We realized that during target motion eccentricity-dependent representation biases could also influence the interception errors (Brooks & Mather, 2000; Johnston & Wright, 1986; Neppi-Mòdona et al., 2004; Tynan & Sekuler, 1982). As will be shown next, such biases would introduce an error that depends on the initial IP eccentricity. In line with the analyses above, the gaze-centered representation of the IP would be represented as

$$IP_{GC} = a(IP - FP_A), \quad (A5)$$

where $a \neq 1$ implies a representation bias. As before, the updating process involves subtracting the saccade amplitude:

$$IP_{GC} = a(IP - FP_A) - (FP_B - FP_A). \quad (A6)$$

Transformation biases arise during the transformation into body-centered coordinates:

$$\begin{aligned} IP_{BC} &= a(IP - FP_A) - (FP_B - FP_A) + FP_B \\ &\quad + b(IP - FP_B). \end{aligned} \quad (A7)$$

This yields the following interception error:

$$\text{Error}_{BC} = (a - 1)(IP - FP_A) + b(IP - FP_B). \quad (A8)$$

Equation A8 shows that a combination of representation and transformation biases during manual interception

would yield mixed effects of the initial and final IP eccentricities on the interception errors.

Acknowledgments

Commercial relationships: none.

Corresponding author: Joost C. Dessing.

Email: joost@yorku.ca.

Address: Centre for Vision Research, York University, CSE Building, Room 0003K, 4700 Keele Street, Toronto, M3J 1P3 Ontario, Canada.

Footnotes

¹It should be noted that the summed interception errors for the two *fixation* trials ($T_A + T_B$) should also be predictable from the summed interception errors for the *saccade* trials ($\beta T_A + (1 - \beta)T_B + \beta T_B + (1 - \beta)T_A = T_A + T_B$) if there are pre- and post-saccadic transformation biases. This possibility, however, is uniquely tested using the relationship between interception errors in saccade trials and the weighted average of the errors in the associated fixation trials. Moreover, this relationship should not explain a lot of variance if there are combined pre-saccadic representation biases and post-saccadic transformation biases.

²Note that this comparison does not suffer from the different number of parameters in the models for the *fixation* and *saccade conditions*, because it is not the explanatory value of the actual regression models that is compared here.

References

- Assad, J. A., & Maunsell, J. H. (1995). Neuronal correlates of inferred motion in primate posterior parietal cortex. *Nature*, 373, 518–521. [PubMed]
- Baker, J. T., Harper, T. M., & Snyder, L. H. (2003). Spatial memory following shifts of gaze: I. Saccades to memorized world-fixed and gaze-fixed targets. *Journal of Neurophysiology*, 89, 2564–2576. [PubMed]
- Batista, A. P., Buneo, C. A., Snyder, L. H., & Andersen, R. A. (1999). Reach plans in eye-centered coordinates. *Science*, 285, 257–260. [PubMed]
- Battaglia-Mayer, A., Caminiti, R., Lacquaniti F., & Zago, M. (2003). Multiple levels of representation of reaching in the parieto-frontal network. *Cerebral Cortex*, 13, 1009–1022. [PubMed]

- Beek, P. J., Dessing, J. C., Peper, C. E., & Bullock, D. (2003). Modelling the control of interceptive actions. *Philosophical Transactions of the Royal Society of London B: Biological Sciences*, 358, 1511–1523. [PubMed]
- Berry, M. J., 2nd, Brivanlou, I. H., Jordan, T. A., & Meister, M. (1999). Anticipation of moving stimuli by the retina. *Nature*, 398, 334–338. [PubMed]
- Beurze, S. M., Toni, I., Pisella, L., & Medendorp, W. P. (2010). Reference frames for reach planning in human parietofrontal cortex. *Journal of Neurophysiology*, 104, 1736–1745. [PubMed]
- Beurze, S. M., Van Pelt, S., & Medendorp, W. P. (2006). Behavioral reference frames for planning human reaching movements. *Journal of Neurophysiology*, 96, 352–362. [PubMed]
- Blakemore, M. R., & Snowden, R. J. (2000). Textured backgrounds alter perceived speed. *Vision Research*, 40, 629–638. [PubMed]
- Blohm, G., & Crawford, J. D. (2007). Computations for geometrically accurate visually guided reaching in 3-D space. *Journal of Vision*, 7(5):4, 1–22, <http://www.journalofvision.org/content/7/5/4>, doi:10.1167/7.5.4. [PubMed] [Article]
- Blohm, G., & Lefèvre, P. (2010). Visuomotor velocity transformations for smooth pursuit eye movements. *Journal of Neurophysiology*, 104, 2103–2115. [PubMed]
- Bock, O. (1986). Contribution of retinal versus extra-retinal signals towards visual localization in goal-directed movements. *Experimental Brain Research*, 64, 476–482. [PubMed]
- Bosco, G., Carrozzo, M., & Lacquaniti, F. (2008). Contributions of the human temporoparietal junction and MT/V5+ to the timing of interception revealed by transcranial magnetic stimulation. *Journal of Neuroscience*, 28, 12071–12084. [PubMed]
- Boulinguez, P., Savazzi, S., & Marzi, C. A. (2009). Visual trajectory perception in humans: Is it lateralized? Clues from online rTMS of the middle-temporal complex (MT/V5). *Behavioural Brain Research*, 197, 481–486. [PubMed]
- Boussaoud, D., Ungerleider, L. G., & Desimone, R. (1990). Pathways for motion analysis: Cortical connections of the medial superior temporal and fundus of the superior temporal visual areas in the macaque. *Journal of Comparative Neurology*, 296, 462–495. [PubMed]
- Bremmer, F., Pouget, A., & Hoffmann, K. P. (1998). Eye position encoding in the macaque posterior parietal cortex. *European Journal of Neuroscience*, 10, 153–160. [PubMed]
- Brenner, E., & Smeets, J. B. (1994). Different frames of reference for position and motion. *Naturwissenschaften*, 81, 30–32. [PubMed]
- Brooks, K., & Mather, G. (2000). Perceived speed of motion in depth is reduced in the periphery. *Vision Research*, 40, 3507–3516. [PubMed]
- Brouwer, A. M., Middelburg, T., Smeets, J. B., & Brenner, E. (2003). Hitting moving targets: A dissociation between the use of the target's speed and direction of motion. *Experimental Brain Research*, 152, 368–375. [PubMed]
- Brouwer, A. M., Smeets, J. B., & Brenner, E. (2005). Hitting moving targets: Effects of target speed and dimensions on movement time. *Experimental Brain Research*, 165, 28–36. [PubMed]
- Byrne, P. A., Cappadocia, D. C., & Crawford, J. D. (2010). Interactions between gaze-centered and allocentric representations of reach target location in the presence of spatial updating. *Vision Research*, 50, 2661–2670. [PubMed]
- Carrozzo, M., McIntyre, J., Zago, M., & Lacquaniti, F. (1999). Viewer-centered and body-centered frames of reference in direct visuomotor transformations. *Experimental Brain Research*, 129, 201–210. [PubMed]
- Cavada, C., & Goldman-Rakic, P. S. (1989). Posterior parietal cortex in rhesus monkey: I. Parcellation of areas based on distinctive limbic and sensory corticocortical connections. *Journal of Comparative Neurology*, 287, 393–421. [PubMed]
- Colby, C. L., Gattass, R., Olson, C. R., & Gross, C. G. (1998). Topographical organization of cortical afferents to extrastriate visual area PO in the macaque: A dual tracer study. *Journal of Comparative Neurology*, 269, 392–413. [PubMed]
- Crawford, J. D., Henriques, D. Y., & Medendorp, W. P. (2011). Three-dimensional transformations for goal-directed action. *Annual Review of Neuroscience*, 34, 309–331. [PubMed]
- Crawford, J. D., Medendorp, W. P., & Marotta, J. J. (2004). Spatial transformations for eye–hand coordination. *Journal of Neurophysiology*, 92, 10–19. [PubMed]
- d'Avossa, G., Tosetti, M., Crespi, S., Biagi, L., Burr, D. C., & Morrone, M. C. (2007). Spatiotopic selectivity of BOLD responses to visual motion in human area MT. *Nature Neuroscience*, 10, 249–255. [PubMed]
- Dessing, J. C., Crawford, J. D., & Medendorp, W. P. (2010). *Testing the spatial reference frames used for manual interception*. Poster presented at the 10th Annual Meeting of the Vision Sciences Society. [Abstract]

- Dessing, J. C., Oostwoud Wijdenes, L., Peper, C. E., & Beek, P. J. (2009a). Adaptations of lateral hand movements to early and late visual occlusion in catching. *Experimental Brain Research*, 192, 511–527. [PubMed]
- Dessing, J. C., Oostwoud Wijdenes, L., Peper, C. E., & Beek, P. J. (2009b). Visuomotor transformation for interception: Catching while fixating. *Experimental Brain Research*, 196, 511–527. [PubMed] [Article]
- Dessing, J. C., Peper, C. E., Bullock, D., & Beek, P. J. (2005). How position, velocity, and temporal information combine in the prospective control of catching: Data and model. *Journal of Cognitive Neuroscience*, 17, 668–686. [PubMed]
- Duhamel, J. R., Bremmer, F., BenHamed, S., & Graf, W. (1997). Spatial invariance of visual receptive fields in parietal cortex neurons. *Nature*, 389, 845–848. [PubMed]
- Enright, J. T. (1995). The non-visual impact of eye orientation on eye–hand coordination. *Vision Research*, 35, 1611–1618. [PubMed]
- Fiehler, K., Rösler, F., & Henriques, D. Y. (2010). Interaction between gaze and visual and proprioceptive position judgements. *Experimental Brain Research*, 203, 485–498. [PubMed]
- Galletti, C., Fattori, P., Kutz, D. F., & Gamberini, M. (1999). Brain location and visual topography of cortical area V6A in the macaque monkey. *European Journal of Neuroscience*, 11, 575–582. [PubMed]
- Galletti, C., Gamberini, M., Kutz, D. F., Baldinotti, I., & Fattori, P. (2005). The relationship between V6 and PO in macaque extrastriate cortex. *European Journal of Neuroscience*, 21, 959–970. [PubMed]
- Gardner, J. L., Merriam, E. P., Movshon, J. A., & Heeger, D. J. (2008). Maps of visual space in human occipital cortex are retinotopic, not spatiotopic. *Journal of Neuroscience*, 28, 3988–3999. [PubMed] [Article]
- Harris, J. M., & Dean, P. J. A. (2003). Accuracy and precision of binocular 3-D motion perception. *Journal of Experimental Psychology: Human Perception and Performance*, 29, 869–881. [PubMed]
- Henriques, D. Y. P., & Crawford, J. D. (2000). Direction-dependent distortions of retinocentric space in the visuomotor transformation for pointing. *Experimental Brain Research*, 132, 179–194. [PubMed]
- Henriques, D. Y. P., Klier, E. M., Smith, M. A., Lowy, D., & Crawford, J. D. (1998). Gaze-centered remapping of remembered visual space in an open-loop pointing task. *Journal of Neuroscience*, 18, 1583–1594. [PubMed]
- Heuer, H., & Sangals, J. (1998). Task-dependent mixtures of coordinate systems in visuomotor transformations. *Experimental Brain Research*, 119, 224–236. [PubMed]
- Ilg, U. J., & Schumann, S. (2007). Primate area MST-l is involved in the generation of goal-directed eye and hand movements. *Journal of Neurophysiology*, 97, 761–771. [PubMed]
- Ilg, U. J., Schumann, S., & Thier, P. (2004). Posterior parietal cortex neurons encode target motion in world-centered coordinates. *Neuron*, 43, 145–151. [PubMed]
- Inaba, N., Shinomoto, S., Yamane, S., Takemura, A., & Kawano, K. (2007). MST neurons code for visual motion in space independent of pursuit eye movements. *Journal of Neurophysiology*, 97, 3473–3483. [PubMed]
- Johnston, A., & Wright, M. J. (1986). Matching velocity in central and peripheral vision. *Vision Research*, 26, 1099–1109. [PubMed]
- Jones, S. A., & Henriques, D. Y. (2010). Memory for proprioceptive and multisensory targets is partially coded relative to gaze. *Neuropsychologia*, 48, 3782–3792. [PubMed]
- Khan, A. Z., Crawford, J. D., Blohm, G., Urquizar, C., Rossetti, Y., & Pisella, L. (2007). Influence of initial hand and target position on reach errors in optic ataxic and normal subjects. *Journal of Vision*, 7(5):8, 1–16, <http://www.journalofvision.org/content/7/5/8>, doi:10.1167/7.5.8. [PubMed] [Article]
- Khan, A. Z., Pisella, L., Rossetti, Y., Vighetto, A., & Crawford, J. D. (2005). Impairment of gaze-centered updating of reach targets in bilateral parietal-occipital damaged patients. *Cerebral Cortex*, 15, 1547–1560. [PubMed]
- Khan, A. Z., Pisella, L., Vighetto, A., Cotton, F., Luauté, J., Boisson, D., et al. (2005). Optic ataxia errors depend on remapped, not viewed, target location. *Nature Neuroscience*, 8, 418–420. [PubMed]
- Krauzlis, R. J. (2004). Recasting the smooth pursuit eye movement system. *Journal of Neurophysiology*, 91, 591–603. [PubMed]
- Krekelberg, B., Kubischik, M., Hoffmann, K. P., & Bremmer, F. (2003). Neural correlates of visual localization and perisaccadic mislocalization. *Neuron*, 37, 537–545. [PubMed]
- Lemay, M., & Stelmach, G. E. (2005). Multiple frames of reference for pointing to a remembered target. *Experimental Brain Research*, 164, 301–310. [PubMed]
- Martinez-Trujillo, J. C., Medendorp, W. P., Wang, H., & Crawford, J. D. (2004). Frames of reference for eye–head gaze commands in primate supplementary eye fields. *Neuron*, 44, 1057–1066. [PubMed]

- Marzocchi, N., Breveglieri, R., Galletti, C., & Fattori, P. (2008). Reaching activity in parietal area V6A of macaque: Eye influence on arm activity or retinocentric coding of reaching movements? *European Journal of Neuroscience*, 27, 775–789. [PubMed]
- McBeath, M. K., Shaffer, D. M., & Kaiser, M. K. (1995). How baseball outfielders determine where to run to catch fly balls. *Science*, 268, 569–573. [PubMed]
- McGuire, L. M., & Sabes, P. N. (2009). Sensory transformations and the use of multiple reference frames for reach planning. *Nature Neuroscience*, 12, 1056–1061. [PubMed]
- McIntyre, J., Stratta, F., & Lacquaniti, F. (1998). Short-term memory for reaching to visual targets: Psychophysical evidence for body-centered reference frames. *Journal of Neuroscience*, 18, 8423–8435. [PubMed]
- McIntyre, J., Zago, M., Berthoz, A., & Lacquaniti, F. (2001). Does the brain model Newton's laws? *Nature Neuroscience*, 4, 693–694. [PubMed]
- Medendorp, W. P. (2011). Spatial constancy mechanisms in motor control. *Philosophical Transactions of the Royal Society of London B: Biological Sciences*, 366, 476–491. [PubMed]
- Medendorp, W. P., & Crawford, J. D. (2002). Visuospatial updating of reaching targets in near and far space. *Neuroreport*, 13, 633–636. [PubMed]
- Medendorp, W. P., Goltz, H. C., Vilis, T., & Crawford, J. D. (2003). Gaze-centered updating of visual space in human parietal cortex. *Journal of Neuroscience*, 23, 6209–6214. [PubMed]
- Melcher, D., & Morrone, M. C. (2003). Spatiotopic temporal integration of visual motion across saccadic eye movements. *Nature Neuroscience*, 6, 877–881. [PubMed]
- Merchant, H., Battaglia-Mayer, A., & Georgopoulos, A. P. (2004). Neural responses during interception of real and apparent circularly moving stimuli in motor cortex and area 7a. *Cerebral Cortex*, 14, 314–331. [PubMed]
- Merchant, H., Zarco, W., Prado, L., & Pérez, O. (2009). Behavioral and neurophysiological aspects of target interception. *Advances in Experimental Medicine and Biology*, 629, 201–220. [PubMed]
- Morvan, C., & Wexler, M. (2005). Reference frames in early motion detection. *Journal of Vision*, 5(2):4, 131–138, <http://www.journalofvision.org/content/5/2/4>, doi:10.1167/5.2.4. [PubMed] [Article]
- Mullette-Gillman, O. A., Cohen, Y. E., & Groh, J. M. (2005). Eye-centered, head-centered, and complex coding of visual and auditory targets in the intraparietal sulcus. *Journal of Neurophysiology*, 94, 2331–2352. [PubMed]
- Mullette-Gillman, O. A., Cohen, Y. E., & Groh, J. M. (2009). Motor-related signals in the intraparietal cortex encode locations in a hybrid, rather than eye-centered reference frame. *Cerebral Cortex*, 19, 1761–1775. [PubMed]
- Neppi-Mòdona, M., Auclair, D., Sirigu, A., & Duhamel, J. R. (2004). Spatial coding of the predicted impact location of a looming object. *Current Biology*, 14, 1174–1180. [PubMed]
- Oldfield, R. C. (1971). The assessment and analysis of handedness: The Edinburgh inventory. *Neuropsychologia*, 9, 97–113. [PubMed]
- Olson, I. R., Gatenby, J. C., Leung, H. C., Skudlarski, P., & Gore, J. C. (2004). Neuronal representation of occluded objects in the human brain. *Neuropsychologia*, 42, 95–104. [PubMed]
- Ong, W. S., Hooshvar, N., Zhang, M., & Bisley, J. W. (2009). Psychophysical evidence for spatiotopic processing in area MT in a short-term memory for motion task. *Journal of Neurophysiology*, 102, 2435–2440. [PubMed]
- Park, J., Schlag-Rey, M., & Schlag, J. (2006). Frames of reference for saccadic command tested by saccade collision in the supplementary eye field. *Journal of Neurophysiology*, 95, 159–170. [PubMed]
- Peper, C. E., Bootsma, R. J., Mestre, D. R., & Bakker, F. C. (1994). Catching balls: How to get the hand to the right place at the right time. *Journal of Experimental Psychology: Human Perception and Performance*, 20, 591–612. [PubMed]
- Pitzalis, S., Sereno, M. I., Committeri, G., Fattori, P., Galati, G., Patria, F., et al. (2010). Human V6: The medial motion area. *Cerebral Cortex*, 20, 411–424. [PubMed]
- Poljac, E., Neggers, B., & van den Berg, A. V. (2006). Collision judgment of objects approaching the head. *Experimental Brain Research*, 171, 35–46. [PubMed]
- Poljac, E., & van den Berg, A. V. (2003). Representation of heading direction in far and near head space. *Experimental Brain Research*, 151, 501–513. [PubMed]
- Pouget, A., Ducom, J. C., Torri, J., & Bavelier, D. (2002). Multisensory spatial representations in eye-centered coordinates for reaching. *Cognition*, 83, B1–B11. [PubMed]
- Savelsbergh, G. J., Whiting, H. T., & Bootsma, R. J. (1991). Grasping tau. *Journal of Experimental Psychology: Human Perception and Performance*, 17, 315–322. [PubMed]
- Schenk, T., Ellison, A., Rice, N., & Milner, A. D. (2005). The role of V5/MT+ in the control of catching movements: An rTMS study. *Neuropsychologia*, 43, 189–198. [PubMed]

- Scherberger, H., Goodale, M. A., & Andersen, R. A. (2003). Target selection for reaching and saccades share a similar behavioral reference frame in the macaque. *Journal of Neurophysiology*, 89, 1456–1466. [PubMed]
- Senot, P., Baillet, S., Renault, B., & Berthoz, A. (2008). Cortical dynamics of anticipatory mechanisms in interception: A neuromagnetic study. *Journal of Cognitive Neuroscience*, 20, 1827–1838. [PubMed]
- Shuwairi, S. M., Curtis, C. E., & Johnson, S. P. (2007). Neural substrates of dynamic object occlusion. *Journal of Cognitive Neuroscience*, 19, 1275–1285. [PubMed]
- Siegel, R. M. (1998). Representation of visual space in area 7a neurons using the center of mass equation. *Journal of Computational Neuroscience*, 5, 365–381. [PubMed]
- Smeets, J. B. J., & Brenner, E. (1995). Perception and action are based on the same visual information: Distinction between position and velocity. *Journal of Experimental Psychology: Human Perception and Performance*, 21, 19–31. [PubMed]
- Soechting, J. F., Engel, K. C., & Flanders, M. (2001). The Duncker illusion in eye–hand coordination. *Journal of Neurophysiology*, 85, 843–854. [PubMed]
- Soechting, J. F., & Flanders, M. (2008). Extrapolation of visual motion for manual interception. *Journal of Neurophysiology*, 99, 2956–2967. [PubMed]
- Sorrento, G. U., & Henriques, D. Y. (2008). Reference frame conversions for repeated arm movements. *Journal of Neurophysiology*, 99, 2968–2984. [PubMed]
- Stricanne, B., Andersen, R. A., & Mazzoni, P. (1996). Eye-centered, head-centered, and intermediate coding of remembered sound locations in area LIP. *Journal of Neurophysiology*, 76, 2071–2076. [PubMed]
- Thompson, A. A., & Henriques, D. Y. P. (2009). *Pointing target locations are updated online in eye-fixed coordinates*. Paper presented at the 20th Neural Control of Movement Annual Conference.
- Tynan, P. D., & Sekuler, R. (1982). Motion processing in peripheral vision: Reaction time and perceived velocity. *Vision Research*, 22, 61–68. [PubMed]
- Ungerleider, L. G., & Desimone, R. (1986). Cortical connections of visual area MT in the macaque. *Journal of Comparative Neurology*, 248, 190–222. [PubMed]
- Van Pelt, S., & Medendorp, W. P. (2007). Gaze-centered updating of remembered visual space during active whole-body translations. *Journal of Neurophysiology*, 97, 1209–1220. [PubMed]
- Van Pelt, S., & Medendorp, W. P. (2008). Updating target distance across eye movements in depth. *Journal of Neurophysiology*, 99, 2281–2290. [PubMed]
- Vaziri, S., Diedrichsen, J., & Shadmehr, R. (2006). Why does the brain predict sensory consequences of oculomotor commands? Optimal integration of the predicted and the actual sensory feedback. *Journal of Neuroscience*, 26, 4188–4197. [PubMed]
- Vesia, M., Prime, S., Yan, X., Sergio, L. E., & Crawford, J. D. (2010). Specificity of human parietal saccade and reach regions during transcranial magnetic stimulation. *Journal of Neuroscience*, 30, 13053–13065. [PubMed]
- Welchman, A. E., Harris, J. M., & Brenner, E. (2009). Extra-retinal signals support the estimation of 3D motion. *Vision Research*, 49, 782–789. [PubMed]
- Welchman, A. E., Tuck, V. L., & Harris, J. M. (2004). Human observers are biased in judging the angular approach of a projectile. *Vision Research*, 44, 2027–2042. [PubMed]
- Wenderoth, P., & Wiese, M. (2008). Retinotopic encoding of the direction aftereffect. *Vision Research*, 48, 1949–1954. [PubMed]
- York, D. (1966). Least-squares fitting of a straight line. *Canadian Journal of Physics*, 44, 1079–1086. [Abstract]
- Zago, M., McIntyre, J., Senot, P., & Lacquaniti, F. (2009). Visuo-motor coordination and internal models for object interception. *Experimental Brain Research*, 192, 571–604. [PubMed]